Pis'ma v ZhETF, vol. 89, iss. 4, pp. 236 – 239

Dependence of transport through carbon nanotubes on local Coulomb potential

A. A. Zhukov, G. Finkelstein+

Institute of Solid State Physics RAS, 142432 Chernogolovka, Russia

+*Department of Physics, Duke University, Durham, North Carolina 27708, USA*

Submitted 22 January 2009

In this paper, we present the results of helium temperature transport measurements through carbon nanotubes using an AFM conductive tip as a mobile gate for creation of a local distributive Coulomb potential. In semiconducting nanotubes we observe shifting of the conductance peaks with changing of the AFM tip position. This result can be explained with a particle in the box quantum model. In high quality metallic nanotubes we observe that the local Coulomb potential does not destroy the fourfold degeneracy of the energy levels.

PACS: 71.20.Tx, 73.23.Hk, 73.63.Fg

The electronic properties of carbon nanotubes have been of interest since their discovery [1]. Quantum dots made from carbon nanotube have a large energy scale due the quantization around the nanotube and the additional quantization along the nanotube length. The fourfold degeneracy of energy levels is expected from the band structure [2] of metallic nanotubes. This degeneracy can be observed in the grouping of conductance peaks in four-peaks clusters [3, 4]. Nanotubes that have defects or charge impurities are not expected to show four-fold degeneracy. Two peaks clusters of spin degenerate energy states have been found in suspended semiconductor nanotubes [5].

One of the most powerful methods to observe the influence of defects on nanotube conductivity is scanned gate microscopy [6 – 8]. Until now, most scanned gate microscopy experiments have been performed at room temperatures [6, 7]. Only one experiment has been reported at low temperatures ($T = 0.6$ K) [8], no degeneracy of energy levels in conductance peaks was reported.

In this paper we present the results of our low temperature scanned gate microscopy (SGM). Specifically, we tuned the local Coulomb potential with our conductive AFM tip while we carried out transport measurements through semiconducting, and high quality metallic, carbon nanotubes at $T = 4.5$ K. Our results will concentrate on conductance peaks positions and the fourfold degeneracy of energy levels in the presence of an external potential.

The nanotubes used in this experiment were grown by a CVD method using CO as the feedstock gas. The details of this process are described elsewhere [9]. The contacts to the nanotubes were defined with e-beam lithography. The semiconducting nanotube (Sample 1), was connected with evaporated Cr/Au contacts, and, the metallic nanotube (Sample 2), was connected with evaporated Pd/Au contacts. Additionally, search patterns around the sample were made to aid in the location of the tube at helium temperatures. An AFM image taken at 77 K of a typical device is shown in Fig.1a, b illustrates the general measurement setup of experiment. The AFM used in our experiment is home made, with a mechanical positioning range of approximately $(1\,\text{mm})^2$ and a scanning range of $(2.5\,\mu\text{m})^2$ at helium temperatures. All results shown in this paper were measured at $T = 4.5$ K.

The insert in Fig.2a shows a SGM image of Sample 1, obtained at $V_{BG} = 0$ V and $V_t = -2.7$ V, the dark spots represent regions of higher conductivity. The line parallel to the tube shows the path of tip movement. The distance to the tube was maintained at a constant ($d = 1.0\,\mu$m). Fig.2a shows dependence of the conductivity of semiconducting nanotube on back gate voltage (V_{BG}), $V_t = -2.7$ V. The differential conductance was measured by standard AC technique with an excitation voltage of 0.1 mV RMS. Each curve was obtained at a different tip position (as shown in the insert of Fig.2a). The results have been shifted (by less then V_{BG} =0.1 V), to make the conductance peaks below -3.75 V coincide. The first conductance peaks of holes in the valence band start to appear at $V_{BG} < -2.25$ V. It can be seen that for the first few hole states the position of Coulomb blockade peaks depends on tip position while for the back gate values below -3.75 V tip displacement is not so significant (ie. the gaps between the peaks do not change).

Fig.3 shows a scanned gate image of a high quality metallic tube, $V_t = -8$ V, $V_{BG} = 0$ V. It is easy to see that the equipotential lines show fourfold grouping when

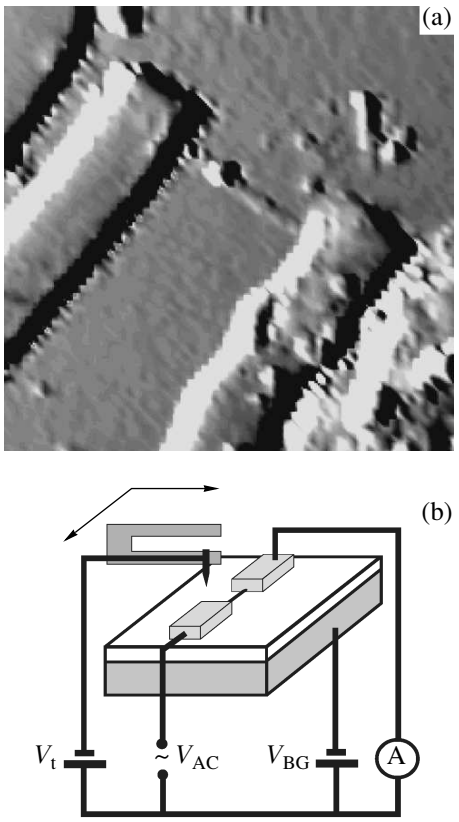

Fig.1. (a) AFM image of typical device used in experiment made at $T = 77$ K; (b) Electrical scheme of experiment, V_{BG} – back gate voltage, V_t – tip voltage [11]

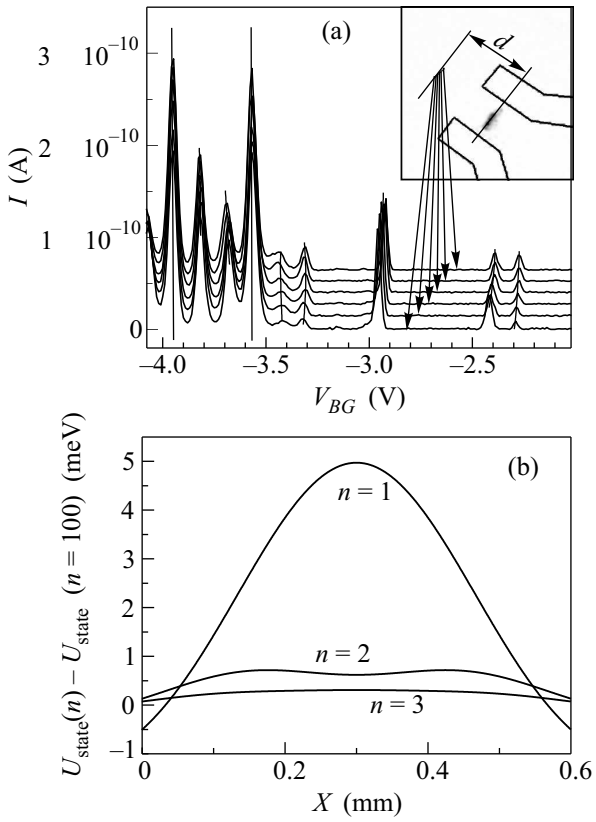

Fig.2. (a) Conductivity vs back gate voltage of semiconducting tube, $V_t = -2.7$ V. Insertion: scanning gate image of Sample 1, obtained at $V_{BG} = 0$ V and $V_t = -2.7$ V, conductive regions are dark. Distance between tube and line of AFM tip movement $d = 1.0\,\mu$m, length of tube $l \simeq 0.6\,\mu$m. Metallic contacts are drawn by solid lines, position of tube and line of tip movement marked by dashed line. (b) Calculated of shifts of peak positions for n =0, 1, 2, shift of energy level for n =100 is subtracted, distance between tube and line of AFM tip movement $d = 0.3\,\mu$m. Color online

the tip is far from the nanotube. To ascertain the influence of the local Coulomb potential close to the nanotube we measured differential conductance versus back gate voltage while moving tip along an equipotential line, the dotted line in Fig.3. The results of this measurements can be seen in Fig.4. The differential conductance was measured by a standard AC technique with an excitation voltage of 1 mV RMS. The conductance peaks positions do not change and their grouping in four peak clusters can be seen for all ten curves, although the heights of the peaks change dramatically. Thus, we seen no effect on the fourfold energy level degeneracy due to the local Coulomb potential.

The energy levels shifts in the case of the semiconducting nanotube can be explained qualitatively in the framework of the "particle in a 1-D box" model. Half the wavelength of the hole wave function is equal to l/n where l is the length of the tube and n is the state number position. When the first holes fill the nanotube nodes of their wave functions shift considerably ($\delta l \sim d$ where d is distance between tube and line of tip movement, see Fig.2a insertion) for each filling state. This results in measurable deviation of the energy gap in between conductance peaks for states with low n.

We perform calculations of shifting of energy levels due to tip displacement. We assume that our tip has a shape of ball [7] with radius of $r_t = 100$ nm and potential of $V_t = -2.7$ V. Including screening from doped back gate placed δz=1 μm beneath the nanotube we can find

$$U_{\text{state}}(n, x_0) = \frac{2V_t r_t \beta}{1+\varepsilon} \int_0^l dx \sin^2(k_n x) \times$$
$$\times \left[\frac{1}{\sqrt{(x_0 - x)^2 + d^2}} - \frac{1}{\sqrt{(x_2 - x)^2 + d^2 + 4\delta z^2}} \right], \quad (1)$$

where $\varepsilon = 3.9$ is the dielectric constant of SiO_2 substrate, $\beta = c_t/c_{BG} = 0.7$ is geometric factor (c_t is ca-

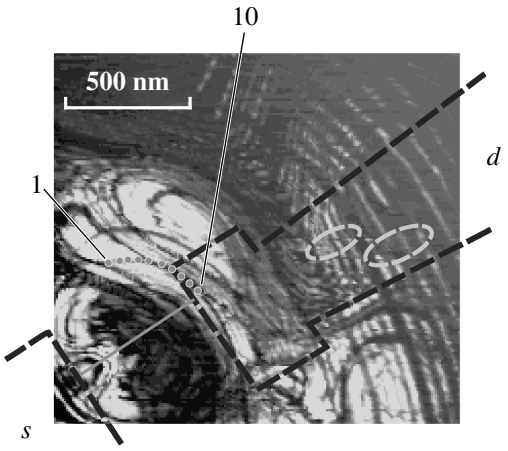

Fig.3. Scanning gate image of high quality metallic nanotube. Back gate voltage $V_{BG} = 0$ V, tip voltage $V_t = -8$ V. More conductive regions are bright. Circles mark 4-line groups. Dots are positions 1 to 10 of tip for conductivity vs back gate measurements, see Fig.4. Color online

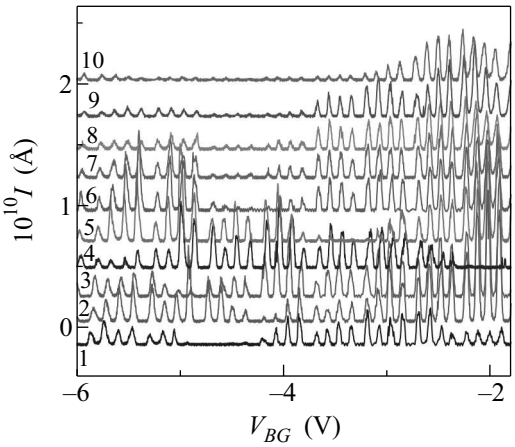

Fig.4. Set of curves 1-10 of conductivity vs back gate voltage, $V_t = -8$ V. Tip positions are marked in Fig.3. Color online

pacitance in between tip and nanotube and c_{BG} is capacitance in between tip and back gate), $k_n = \pi n/l$ is wave vector of electron or hall wave function. Additional spacial variation of U_{state} induced by metallic contacts of the nanotube is not taken into account. Calculated values of energy levels shifts due to charged tip movement (see Fig.2b) are comparable with experimental data (Fig.2a) if we assume distance in between tip and nanotube $d = 0.3$ μm which is significantly smaller than we have in experiment. The reason of such discrepancy is not clear so only the general behavior of shifting of calculated energy levels positions coincide with ones observed experimentally.

In the case of a metallic nanotube all states within the back gate voltage under investigation are low-lying states (n is large). This partly resembles the situation with low-lying states in semiconducting nanotube so survival of 4-peaks clusters at first glance looks rather reasonable. But the local Coulomb potential not only changes the potential of the nanotube itself but also the opacity of the potential barriers in between nanotube and contacts. This is clearly visible in Fig.3 as the Coulomb peaks heights change. So we see that the deviation of coupling strength of tube to the contacts does not effect the stability of the fourfold degenerated states.

The influence of Coulomb impurities, defects of the carbon nanotube and the role of the ends of nanotube have been studied in the theoretical work of San-Huang Ke *et al.* [10]. In this paper the authors performed numerical calculations using density-functional theory of additional energy spectra for quantum dots made of ideal nanotubes of various length, nanotubes with (5-7-7-5) defects and ideal nanotube with Coulomb impurities. This paper suggests that in an ideal nanotube, Coulomb impurities are insignificant and do not change additional energy and thus, do not effect fourfold degeneracy. These theoretical predictions are in good agreement with our experimental data for low lying states in high quality metallic nanotube. From the experimental data presented in Fig.3 and 4 we can conclude, following paper [10], that only the imperfections or defects of tube itself (such as 5-7-7-5) can destroy fourfold degeneracy of the energy states in metallic carbon nanotubes.

In conclusion, we performed transport measurements of semiconducting and metallic carbon nanotubes with external tunable Coulomb potential created by a conductive AFM tip. Shifting of the conductance peaks positions for the first hole states is observed and explained qualitatively in framework of particle in 1D box model for semiconducting nanotubes. Stability of the fourfold degeneracy of the energy states in a metallic nanotube to external Coulomb potential and coupling to the contacts is demonstrated. These observations are in agreement with previous theoretical calculations where no influence of local Coulomb potential and the opacity of potential barriers on degenerate states has been found. Thus, we can conclude that destruction of the fourfold degeneration only comes from defects and imperfections of the metallic nanotube itself.

This work is supported by Russian Foundation for Basic Research, programs of the Russian Academy of Science, and the Program for Support of Leading scientific Schools. We thank A. Makarovsky for help with samples preparation.

1. S. Iijima, Nature **354**, 56 (1991).
2. M. S. Dresselhaus, G. Dresselhaus, and P. C. Eklund, *Science of Fullerence and Carbon Nanotubes*, Academic, San Diego, 1996.
3. W. Liang, M. Bockrath, and H. Park, Phys. Rev. Lett. **88**, 126801 (2003).
4. A. Makarovski, A. Zhukov, L. An et al., arXiv cond-mat/0508401 (2005).
5. P. Jarillo-Herrero, S. Sapmaz, C. Dekker et al., Nature **429**, 389 (2004).
6. S. J. Tans and C. Dekker, Nature **404**, 834 (2000); M. Bockrath, W. Liang, D. Bozovic et al., Science **291**, 283 (2001); S. V. Kalinin, D. A. Bonnell, M. Freitag, and A. T. Johnson, Appl. Phys. Lett. **81**, 5219 (2002).
7. M. Freitag, A. T. Johnson, S. V. Kalinin, and D. A. Bonnell, Phys. Rev. Lett. **89**, 216801 (2002).
8. M. T. Woodside and P. L. McEuen, Science **296**, 1098 (2002).
9. B. Zheng, C. Lu, G. Gu et al., Nano Lett. **2**, 895 (2002).
10. San-Huang Ke, H. U. Baranger, and W. Yang, Phys. Rev. Lett. **91**, 116803 (2003).
11. V_t is not actually the voltage applied to the tip. We use conductive tip made of tungsten wire and it is known that the end of the tip is covered by oxide which could make an additional correction of the tip potential. So the value of V_t we presented is the real potential obtained experimentally from Kelvin probe measurements (Sample 2) or extracting this value from additional set of experiments (Sample 1).